AGU PUBLICATIONS

Water Resources Research

RESEARCH ARTICLE
10.1002/2017WR021502

Time-Variable Transit Time Distributions in the Hyporheic Zone of a Headwater Mountain Stream

Adam S. Ward[1], Noah M. Schmadel[1,2], and Steven M. Wondzell[3]

[1]School of Public and Environmental Affairs, Indiana University, Bloomington, IN, USA, [2]Now at U.S. Geological Survey, Reston, VA, USA, [3]United States Department of Agriculture, Pacific Northwest Research Station, Forest Service, Corvallis, OR, USA

Key Points:
- Hyporheic transit time distributions are more variable in space than in time
- Transit time distributions are not transferrable during periods of rapid changes in stream discharge
- Relatively short study reaches may not capture representative spatial variation along a study reach

Supporting Information:
- Supporting Information S1

Correspondence to:
A. S. Ward,
adamward@indiana.edu

Citation:
Ward, A. S., Schmadel, N. M., & Wondzell, S. M. (2018). Time-variable transit time distributions in the hyporheic zone of a headwater mountain stream. *Water Resources Research*, *54*, 2017–2036. https://doi.org/10.1002/2017WR021502

Received 11 JUL 2017
Accepted 20 FEB 2018
Accepted article online 23 FEB 2018
Published online 23 MAR 2018

Abstract Exchange of water between streams and their hyporheic zones is known to be dynamic in response to hydrologic forcing, variable in space, and to exist in a framework with nested flow cells. The expected result of heterogeneous geomorphic setting, hydrologic forcing, and between-feature interaction is hyporheic transit times that are highly variable in both space and time. Transit time distributions (TTDs) are important as they reflect the potential for hyporheic processes to impact biogeochemical transformations and ecosystems. In this study we simulate time-variable transit time distributions based on dynamic vertical exchange in a headwater mountain stream with observed, heterogeneous step-pool morphology. Our simulations include hyporheic exchange over a 600 m river corridor reach driven by continuously observed, time-variable hydrologic conditions for more than 1 year. We found that spatial variability at an instance in time is typically larger than temporal variation for the reach. Furthermore, we found reach-scale TTDs were marginally variable under all but the most extreme hydrologic conditions, indicating that TTDs are highly transferable in time. Finally, we found that aggregation of annual variation in space and time into a "master TTD" reasonably represents most of the hydrologic dynamics simulated, suggesting that this aggregation approach may provide a relevant basis for scaling from features or short reaches to entire networks.

Plain Language Summary The exchange of water between streams and the shallow subsurface of their valleys is important to ecological functions, many of which depend upon the time it takes water to travel down the valley. For decades, researchers have focused on how river form affects this travel time, leaving a limited understanding of how travel times may change throughout the year due to different wetness conditions. Here we directly address this limitation by estimating travel times through a stream and its entire valley for a period of more than 1 year. We found that change in travel times caused by different wetness conditions throughout the year was smaller than variation caused by river form. Exceptions to this rule are during very dry times of year when streamflow is low or during very wet times of the year when streamflow is high such as those resulting from spring snowmelt flooding.

1. Introduction

Transit times in the hyporheic zone are the time scales over which ecological processes and functions associated with hyporheic exchange can occur (Findlay, 1995; Gooseff et al., 2003; Zarnetske et al., 2011). Thus, prediction of hyporheic transit time distributions (TTDs) is required for prediction of hyporheic functions (Boulton et al., 1998; Brunke et al., 1997; Krause et al., 2011; Merill & Tonjes, 2014). An emerging predictive challenge arises from the growing recognition that these TTDs can be time-variable (Harman et al., 2016). Empirical and numerical studies have documented time-variable TTDs at the reach-scale in response to base flow recession (Ward et al., 2013c, 2017), storm events (Dudley-Southern & Binley, 2015; Ward et al., 2013a), and diurnal fluctuations (Gerecht et al., 2011; Harman et al., 2016; Sawyer et al., 2015; Schmadel et al., 2016a). However, others have observed hyporheic transit times are essentially constant over a wide range of stream discharges (Ward et al., 2016, 2017). Given these conflicting results, it remains unclear how reach-scale TTDs vary in response to hydrologic forcing, and how transferable an observed TTD is to other time periods, stream discharge conditions, and locations.

Hyporheic TTDs reflect interactions between geomorphic setting and dynamic hydrologic forcing (Ward et al., 2012; Wondzell & Gooseff, 2014). Geomorphic setting refers to the relatively static physical system, including the spatial heterogeneity in the hydraulic conductivity field (Packman & Salehin, 2003; Salehin et al., 2004; Sawyer & Cardenas, 2009), streambed morphology (Boano et al., 2014; Kasahara & Wondzell, 2003), lithologic structure (Ryan et al., 2004; Vaux, 1968; Ward et al., 2013b), valley constraint (D'Angelo et al., 1993; Stanford & Ward, 1993; Ward et al., 2016, 2017; Wondzell, 2006; Wright et al., 2005), and geologic parent material (Payn et al., 2009; Valett et al., 1997). Hydrologic forcing occurs at multiple boundaries. First, at the stream-hyporheic interface where stream discharge interacts with streambed morphology to yield changing hydraulic gradients (e.g., Elliott & Brooks, 1997a, 1997b; Stonedahl et al., 2010; Tonina & Buffington, 2009) and diffusion of turbulent momentum across the streambed (Boano et al., 2014; Malzone et al., 2016; Packman et al., 2004). Next, inflows from the hillslopes and groundwater system toward the stream may compress hyporheic zones (e.g., Cardenas & Wilson, 2007a; Storey et al., 2003). These inflows have also been identified as truncating longer down-valley flow paths, forcing them to return to the stream in response to focused upwelling (Schmadel et al., 2017).

Measurement of hyporheic TTDs has been a central focus of many hydrologists given the clear linkage of these TTDs to ecological functions and pollutant legacy (e.g., Fuller & Harvey, 2000; Gandy et al., 2007; Hester & Gooseff, 2010). Indeed, instantaneous tracer injections are directly interpreted as TTDs, and constant rate injections may be deconvolved to provide similar information (e.g., McGuire & McDonnell, 2006; Payn et al., 2008). Such field-based approaches inherently assume that a measured TTD is both representative of the hyporheic zone and can be used as a basis to interpret other associated processes such as nutrient spiraling (e.g., Connor et al., 2010). However, the implicit assumption that a measured TTD is representative across other hydrologic conditions and spatial scales is seldom tested. One strategy to account for time-variable TTDs is to construct composite (or "master") TTDs that integrate all TTDs across a range of hydrologic conditions (Botter et al., 2011; Heidbüchel et al., 2012; Rinaldo et al., 2011). A master TTD is assumed to effectively represent all possible variability of the hyporheic TTD integrated over some time scale, but that assumption has not been tested either. A second strategy is to relate characteristics of the TTD to readily observable hydrologic conditions. For example, Harman et al. (2016) regressed characteristics of their ranked StorAge Selection (rSAS) function against stream discharge, using this regression to simulate a continuously variable TTD along a valley segment. While they showed that younger hyporheic water was more likely to turnover than older hyporheic water during higher stream discharge conditions, it is still not clear what causes variation in TTDs. At present, it is impossible to know if a TTD measured at a single time or place is representative of any other time or place because the interactions between dynamic hydrologic forcing and geomorphic setting are poorly understood. The lack of predictive power ultimately limits our ability to forecast ecosystem response or pollutant legacy, which depend on an approximation of the master TTD at large scales.

Much of our current predictive power is based on studies at the scale of individual features (e.g., individual meander bends or bed forms) under steady discharge conditions. It is commonly assumed that feature-scale studies are representative of aggregated exchange fluxes and time scales across larger spatial scales, where one particular scale or type of feature is assumed to be the dominant driver of hyporheic exchange. Recent upscaling strategies rely upon the linear combination of features to make predictions at the scale of river networks (Gomez-Velez et al., 2015; Gomez-Velez & Harvey, 2014; Kiel & Cardenas, 2014). This is at odds with the Tóthian view of a nested, multiscale groundwater system (Tóth, 1962, 1963) which is central to high-fidelity models of hyporheic exchange (Stonedahl et al., 2010, 2013). Furthermore, scaling attempts currently focus on steady state discharge conditions. As a result, the dynamic transitions of exchange fluxes and time scales in response to hydrologic forcing are omitted. Thus, reach-scale dynamics remain largely unknown, limiting prediction at these larger network scales where hydrologic conditions and geomorphic setting vary widely.

The objectives of this study are (1) to assess the temporal variability of both instantaneous and spatially discrete hyporheic TTDs through a complete annual cycle of hydrologic forcing at the reach-scale; (2) to assess how representative a TTD at a single point in time is of other TTDs through an annual cycle; (3) to assess the suitability of the master TTD to represent all possible time-variable TTDs; and (4) to assess the length of study reach necessary to characterize TTDs. We expect that hyporheic TTDs will be highly variable through a year, given the orders-of-magnitude change in stream discharge accompanied by large changes in lateral

groundwater inflows. We anticipate that transferability on the basis of discharge will be limited because the same discharge is observed, for example, on the rising and falling limbs of a storm where lateral inflows may be different. Instead, we expect transferability to be most accurate across conditions based on the time rate of change of discharge (e.g., rising-limb TTDs are representative of other rising limbs). We expect the master TTD approach to be most suitable during steady state discharge conditions, which are the most frequent conditions in the stream throughout the year. Finally, we expect that the master TTD will be less representative during the less common lowest, highest, and dynamic periods. To achieve our objectives and test our expectations, we simulated a two-dimensional (2-D) profile hyporheic zone along the thalweg of a 600-m long, second-order headwater mountain stream segment. We calculated hyporheic transit times for more than 44 million particles through a 1-year simulation and used these as the basis to test our expectations and realize our objectives.

2. Methods

2.1. Field Site Description and Monitoring

The study site is Watershed 1 (WS01) of the H.J. Andrews Experimental Forest (HJA) in the western Cascades, Oregon, USA (Figure 1a). Our focused study reach is a segment of the valley that is about 600 m in length and includes a highly studied section instrumented with a well network (e.g., Voltz et al., 2013; Wondzell,

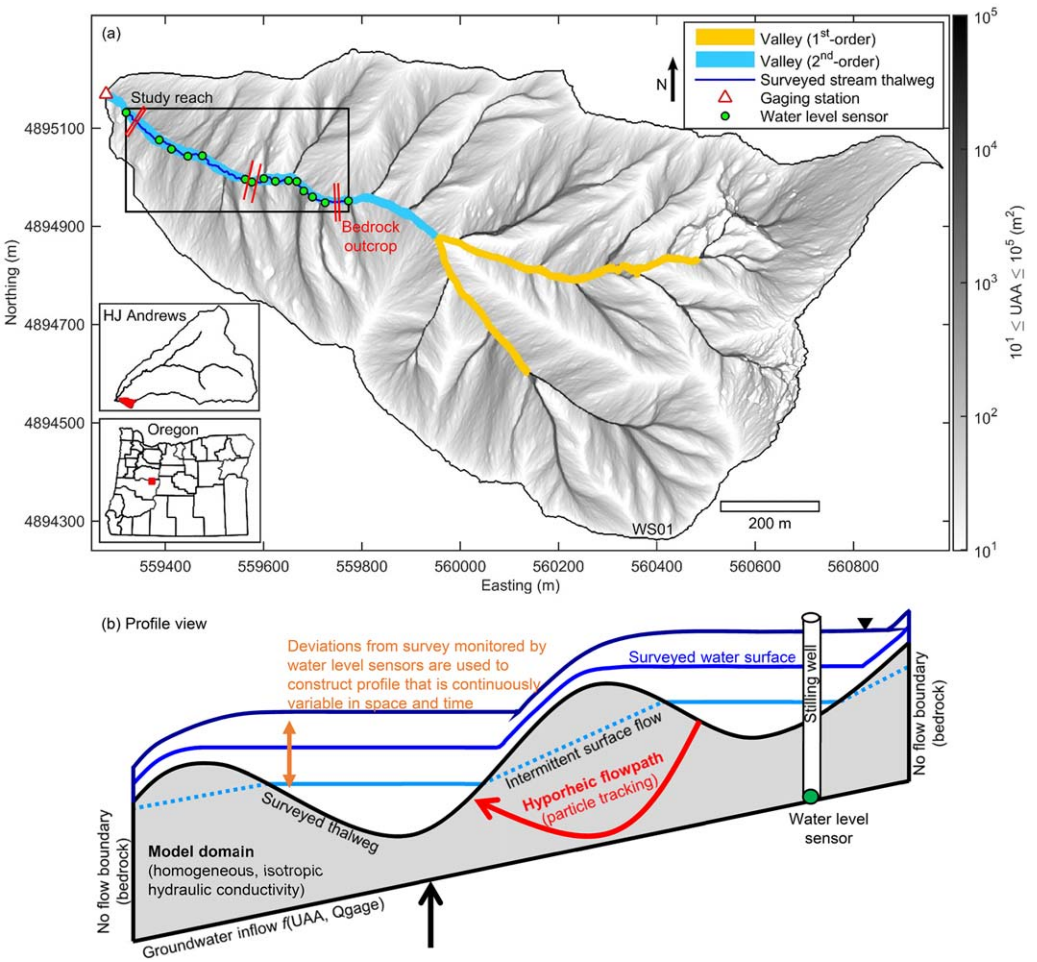

Figure 1. (a) The study site is a 600-m segment of a second-order stream in Watershed 1 (WS01) at the H.J. Andrews Experimental Forest. The location of 15 water level sensors installed along the study reach are shown as are flow lines of the lateral upslope accumulated area (UAA). Darkly shaded areas are deeply incised, narrow channels. (b) Conceptual model of a two-dimensional profile along the stream thalweg in the study reach and implementation of boundaries in the finite element model (modified from Figure 1 in Schmadel et al. (2017), with permission).

2006). The catchment drains about 96 ha of forested land and is characterized by steep hillslopes (>50%) and a steep (~12%), constrained valley bottom averaging about 10.6 m in width (range 2.6–16.8 m along the study reach based on 30 field measurements; Schmadel et al., 2017). The study reach is constrained below by relatively shallow, unweathered bedrock that is exposed at both the upstream and downstream ends and at a few locations near the middle. The stream is gauged about 70 m downstream of the study reach. Precipitation data are from the Primary Meteorological Station at the HJA. Valley bottom colluvium is poorly sorted, deposited as the result of high-energy hillslope failures. Additional details about the HJA and the WS01 field site are presented in several related studies (Dyrness, 1969; Swanson & James, 1975; Swanson & Jones, 2002; Wondzell, 2006).

Most of the longitudinal profile of the stream thalweg and water surface was topographically surveyed on 26–29 May 2015 (average stream discharge 6.7 L s^{-1}); the upstream-most 70 m was surveyed on 26 May 2016 (average stream discharge 5.8 L s^{-1}) (Schmadel et al., 2017) to extend the upstream boundary of the topographic survey to a bedrock outcrop. A total of 15 pressure transducers (HOBO Water Level Data Loggers U20L-04 and U20-001-04, Onset, Bourne, MA) were installed in stilling wells along the study reach and recorded stream stage every 15 min (Figure 1a). Sensors were installed to remain submerged through the low-flow period. Visible inspection confirmed sensors remained submerged, though portions of the streambed did become dry during summer 2016. Finally, lateral upslope accumulated area (UAA) to the valley bottom was tabulated every 1 m along the stream centerline using a one-directional flow accumulation algorithm (Schwanghart & Kuhn, 2010; Schwanghart & Scherler, 2014; Seibert & McGlynn, 2007) as applied to a LiDAR-derived 1-m digital terrain model (Spies, 2016). Additional details of the field campaign are presented by Schmadel et al. (2017).

2.2. Numerical Modeling

The mathematical model implemented is identical to that described by Schmadel et al. (2017), where additional details can be found. The key advance in this study is the implementation of dynamic boundary conditions; Schmadel et al. (2017) limited their analysis to steady state hydrologic conditions. Briefly, the model domain is a 2-D vertical profile along the topographically surveyed stream thalweg. The bottom of the model domain is set at an average of 3 m below the stream (after Gooseff et al., 2006) and planar (i.e., without topography along the bedrock-colluvium interface; after Wondzell et al., 2009). Flow through porous media is simulated using Richards' equation (Richards, 1931). We specified homogeneous and isotropic hydraulic conductivity of 7×10^{-5} m s^{-1}, the geometric mean of falling head tests from WS01 and a nearby paired watershed (Kasahara & Wondzell, 2003), and an effective porosity of 0.2 (Wondzell et al., 2009). We parameterized the Mualem (1976) and Van Genuchten (1980) retention model to generally represent poorly sorted colluvium. Overall, we modeled two reaches in the valley segment separated by an observed bedrock outcrop.

The upstream and downstream boundaries of the two reaches were set as no-flow boundaries based on the observed, intact bedrock outcrops. The bottom boundary was defined as a spatially and temporally variable influx. Inflows to the valley bottom were assigned to 1-m segments along the valley. Inflow for each 1-m segment was based on stream discharge changes proportional to changes in UAA between each segment. This volumetric inflow rate was assigned to the valley bottom area (1 m along the stream centerline by LiDAR-derived valley width) for each segment to estimate vertical fluxes. The streambed boundary was parameterized as a specified head. The series of stage sensors was used to calculate deviations from the surveyed water surface profile. The surveyed profile was adjusted by linearly interpolating the deviations. Using the continuous records of stream discharge at the gauge, the interpolated deviations in stage, UAA, and estimated valley bottom width, flows through both the top (streambed) and bottom (bedrock) boundaries of the model were dynamically adjusted throughout the 1-year simulation period.

The model construction necessarily limits the elements of hydrologic forcing and geologic setting that are considered. For example, our model isolates changing hydrostatic pressure at the streambed and inflows from the hillslope as the dynamic drivers of hyporheic exchange, which are expected to be the dominant mechanisms driving exchange flux in steep headwater streams (e.g., Schmadel et al., 2017; Wondzell & Gooseff, 2013). In lower-gradient systems, other dynamic processes including diffusion of turbulent momentum across the streambed (e.g., Malzone et al., 2016; Packman & Bencala, 2000; Zhou & Mendoza, 1993) and turnover exchange due to moving bed forms (e.g., Elliott & Brooks, 1997a, 1997b). With respect to geologic

setting, this study assumes a homogeneous and isotropic hydraulic conductivity field and a planar interface between colluvium and bedrock, both of which simplify the model construction, but are recognized to impact exchange geometries and time scales (e.g., Salehin et al., 2004; Wondzell et al., 2009).

The computational mesh for the simulation was generated using the general physics meshing algorithm in COMSOL Multiphysics with the preset parameters for a fine mesh. The final mesh for the upper and lower portions of the study segment (separated by exposed bedrock in the channel) consisted of 8,776 elements (average area 0.069 m^2) and 9,195 elements (average area 0.099 m^2), respectively. This exactly matches the mesh of Schmadel et al. (2017).

We simulated the release of massless particles every 10 cm along the streambed (total 5,025 locations) at 1-h intervals for one full year, from 12 June 2015 to 12 June 2016 (total 8,760 release times), for a total of more than 44 million particles released (i.e., at each release time, a total of 5,025 particles were simultaneously released across the reach). Particle tracking was implemented within COMSOL Multiphysics. The position of each particle was tracked each hour and at the time it exited the simulation domain by upwelling back to the stream. We tabulated the time elapsed from particle release to domain exit as the transit time for each particle. Particles were omitted from the analysis if they were released at a location where the streambed was unsaturated or where there was an upwelling flux from the streambed. Thus, only flow paths that are hyporheic (downwelling from the saturated streambed to the subsurface domain and returning to the stream) are included in our analyses. Due to the bedrock constraints, any particle that downwelled eventually returned to the stream. The model simulation period was run for 100 days after the last release to ensure that all particles returned to the stream. Notably, this model formulation limits the analysis to vertical exchange along the stream thalweg, and to those flow paths driven by hydrostatic pressure at the bed. Shorter flow paths, for example those arising due to diffusion of turbulent momentum into the bed or hydraulic jumps, are not included in this study.

2.3. Construction and Analysis of Hyporheic Transit Time Distributions From Particle Tracking Results

2.3.1. Hyporheic Transit Time Distributions

For all TTDs in this study, we constructed empirical TTDs from the transit times of the particles that were simulated. Particles were not flux-weighted in our analyses because we focus specifically on the distributions of transit times in the hyporheic zone (after Schmadel et al., 2016a, 2017; Ward et al., 2011) and those flow paths that are most likely to change in response to hydrologic dynamics. Notably, the resultant impact of these flow paths on, for example, reach transit times that would be observed with tracers or for prediction of ecological function (as in, for example, Gomez-Velez et al., 2015) would require flux-weighted interpretation. Because our focus is on the flow paths themselves and not their aggregate impact on reach-scale transport, we need not flux-weight the distributions. As a result, all TTDs are empirically constructed.

Instantaneous TTDs were constructed by combining transit times from the 5,025 particle release locations along the length of the study reach at each time step (i.e., integrated in space, instantaneous in time). The TTDs were created by first binning the transit times for each release using three bins per order-of-magnitude, and then normalizing the number of particles in each bin by the total number of particles. Thus, the resultant value for each bin represents the relative frequency of transit times for the bin (sum of all values equal to 1). To plot a probability density function (PDF) of the TTD, we assigned the probability calculated for each bin interval to the center of the bin. Thus, all PDFs presented for instantaneous TTDs are empirical, constructed from the tracked particle data and reflecting the unweighted distributions of time scales in the hyporheic zone. We used this methodology to construct an instantaneous TTD for the segment for each hour throughout the 1-year simulation (8,760 total instantaneous TTDs, with each TTD made up of 5,025 particle tracks). For each instantaneous TTD, we tabulated the discharge as the measured gauge discharge at the time of particle release. We also estimated the time rate of change of discharge (dQ/dt) as a predictor variable by smoothing gauged stream discharge using a moving average across a 2-h window, and then tabulated dQ/dt at the time of each instantaneous release time.

Additionally, a series of spatially discrete TTDs were calculated for the maximum, median, and minimum gauge discharge releases. To construct these TTDs, we applied moving spatial windows ranging from 1 to 500 m in length. All particles that both originated and returned to the stream within the moving window were binned using three bins per order-of-magnitude. As with instantaneous TTDs, the bins were normalized by the total number of particles to produce the relative frequency of particles with transit times

between the bin edges and all particles were equally weighted in the analysis. To plot a PDF of the TTD, we assigned the probability calculated for each bin interval to the center of the bin. Thus, all PDFs presented for spatially discrete TTDs are empirical, constructed from the tracked particle data. This spatial subsetting reflects the common field practice of stream solute tracers (e.g., Stream Solute Workshop, 1990), where a selected study reach will not capture underflow (e.g., Harvey et al., 1996; Payn et al., 2009). We calculated the TTDs for all possible moving window locations where at least one flow path originated from and returned to the stream within the moving window.

Finally, a master TTD was constructed by combining every particle released in space and time to produce a single, master TTD, integrating both spatial and temporal variation (after Heidbüchel et al., 2012). To construct a probability density function for the master TTD, we used the same approach as for instantaneous and spatially discrete TTDs (i.e., binned all particles into three bins per order-of-magnitude, normalized by the total number of particles to yield a probability of particles in each bin, particles equally weighted for analysis, plotted by assigning the probabilities to the center of each bin interval). Thus, the PDF presented for the master TTD is empirical, constructed from the tracked particle data. We calculated the cumulative TTD by sorting all particles by transit time and constructing a normalized, cumulative summation:

$$Master_{CDF} = \frac{\sum_{i=1}^{N} T(i)}{N} \tag{1}$$

where $Master_{CDF}$ is the cumulative probability of the sorted TTDs considering all particles released (i.e., the cumulative version of the empirical Master TTD), N is the total number of particles released, and $T(i)$ is the transit time for the ith particle tracked.

2.3.2. Transferability of TTDs in Space and Time

We define the transferability of a TTD as how representative a TTD measured at one time or location is of other times or locations. Specifically, differences between pairs of TTDs were calculated to test how representative an instantaneous TTD is of other times, how representative a spatially discrete TTD is of the complete TTD at a given time step, and how representative the master TTD is of both instantaneous and spatially discrete TTDs. To test transferability of instantaneous TTDs in time, we calculated the root mean square error (RMSE) between all possible pairs of instantaneous TTDs. To test transferability of spatially discrete TTDs, we calculated the RMSE between each spatially discrete TTD and the TTD constructed from all particles released at the time step of interest. Finally, we calculated the RMSE between the master TTD and each instantaneous TTD as:

$$RMSE = \sqrt{\frac{\sum_{i=1}^{N} \left(P_{TTD}(i) - P_{master}(i)\right)^2}{N}} \tag{2}$$

where N is the number of bins used to construct TTDs, $P_{TTD}(i)$ is the probability in the ith bin used to construct the TTDs for each time step, and $P_{master}(i)$ is the probability in the ith bin used to construct the master TTD. We used a similar formulation of calculating RMSE between bin probabilities for the transferability in space and time.

In all cases, we interpret higher RMSE between pairs of TTDs as an indicator of poor transferability, meaning that a TTD from one time or place is not likely to accurately represent a TTD at a different time or place. Because the comparisons are between probability distributions, the units of the calculated RMSE are probability (e.g., RMSE of 0.01 is a mean error of 1% probability across the distribution).

2.3.3. Statistical Tests to Compare Variation in Space to Variation in Time

Variation in space and time was assessed by comparing the coefficient of variation (CV) for each spatial location or time step, calculated as:

$$CV = \frac{\sigma}{\mu} \tag{3}$$

where σ is the standard deviation of transit times calculated for all time steps at a place or spatial locations at a time, and μ is the arithmetic mean for the same data used to calculate σ. The CV represents a measure of spread relative to the mean value.

To compare TTD variation in space to TTD variation in time, we treat the CV for each instantaneous TTD as one sample population, and the CV for each spatially discrete TTD as the second sample population. We

compare the sample populations using a standard one-way analysis of variance (ANOVA), a nonparametric Kruskal-Wallis ANOVA, and a Mann-Whitney-Wilcoxon rank sum test. For all comparisons, we consider $p < 0.05$ to indicate a statistically significant difference between variation in space and time.

2.4. Experimental Field Data as Comparison to Simulations

We compared simulated transit time distributions with those measured in a series of stream solute tracer studies conducted through base flow recession in 2012 (discharge ranging from 38.5 to 1.8 L s^{-1} at the WS01 gauge). These experiments are detailed extensively in related publications (Voltz et al., 2013; Ward et al., 2016, 2017). Briefly, a series of four 48-h constant rate injections of sodium chloride into the stream were conducted about 200 m upstream of the gauging station and monitored both in-stream and in a network of shallow monitoring wells detailed in Wondzell (2006). For observations in the monitoring well network, we used the hyporheic travel times reported by Ward et al. (2017) who separated transit times in the stream from those in the hyporheic zone. We note here these travel times are from the stream to the observation well, meaning they are truncated (assuming random truncation, these should average 50% of the true hyporheic transit times).

For in-stream observations, we used solute tracer time series measured at the well-mixed location about 10 m downstream of the injection location and at the downstream end of our modeled study reach. Background corrected tracer time series were analyzed using the time domain smoothing deconvolution scheme of Cirpka et al. (2007) following the implementation of Payn et al. (2008). We determined the maximum limit for the temporal domain for each injection by increasing the maximum time scale until the probability at the latest time was near-zero, indicating the transfer function is fully contained within the time scale selected. The result of the deconvolution is a transfer function describing the time scales for an instantaneous release into the stream channel at the upstream monitoring location to reach the downstream monitoring location, including advective, dispersive, and short-term storage processes (i.e., those storage flow paths recovered above detection limits, Ward et al., 2013a). We contend this is a reasonable comparison to qualitatively assess time scales in the system because the short-term storage component is part of the transfer function, though we emphasize here that reach-scale TTDs (which integrate both in-stream and hyporheic transport) are not themselves hyporheic TTDs.

3. Results

Through a 1-year simulation, hyporheic transit times varied in response to changes in stream discharge and lateral inflows (Figure 2). For individual particles, hyporheic transit times range from about 2.3 s to 100 d. For all particles tracked, the overall mean and median transit times are 31.2 h and 9.3 h, respectively.

3.1. Time Variability in Instantaneous Transit Time Distributions

Instantaneous TTDs (Figure 3b, showing data combined along columns in Figure 2a) show strong seasonal trends, with the longest mean transit times and largest standard deviations occurring during the lowest stream discharge conditions (June – September 2015; Figure 2e). Over base flow periods, instantaneous TTDs are almost always bimodal (Figures 3b and 3c). The faster mode is typically between 0.04 and 0.4 h, representing the shorter flow paths that downwell and upwell at the scale of individual features (minimum Q in Figures 3b and 3c). The slower mode is between 10 and 100 h, typically representing flow paths that span multiple features (i.e., underflow; Bencala et al., 1984; Castro & Hornberger, 1991; Ward et al., 2016). Under the lowest discharge conditions, the long down-valley flow paths are not forced to the stream by upwelling groundwater, resulting in an increase in the longest time scale flow paths (more than 1,000 h). In contrast, high discharge conditions are associated with largest inflows through the bottom boundary of the model. These strong upwelling fluxes cause down-valley flow paths to return to the stream, generally truncating the longer time scale flow paths. During periods of rapid increases in discharge, inflows are strong enough to cause the longest transit times to disappear (e.g., rise to maximum Q in Figures 3a–3c). Dynamic simulation results—that the longer time scale flow paths are the most sensitive to changing inflows—are consistent with the steady state simulations of Schmadel et al. (2017). Variation in instantaneous TTDs through the year is generally not explained by discharge (Figure 4c) or dQ/dt (Figure 4d). However, variation was slightly smaller during intermediate discharge conditions, with increased variation at both low and high discharges (Figure 4c).

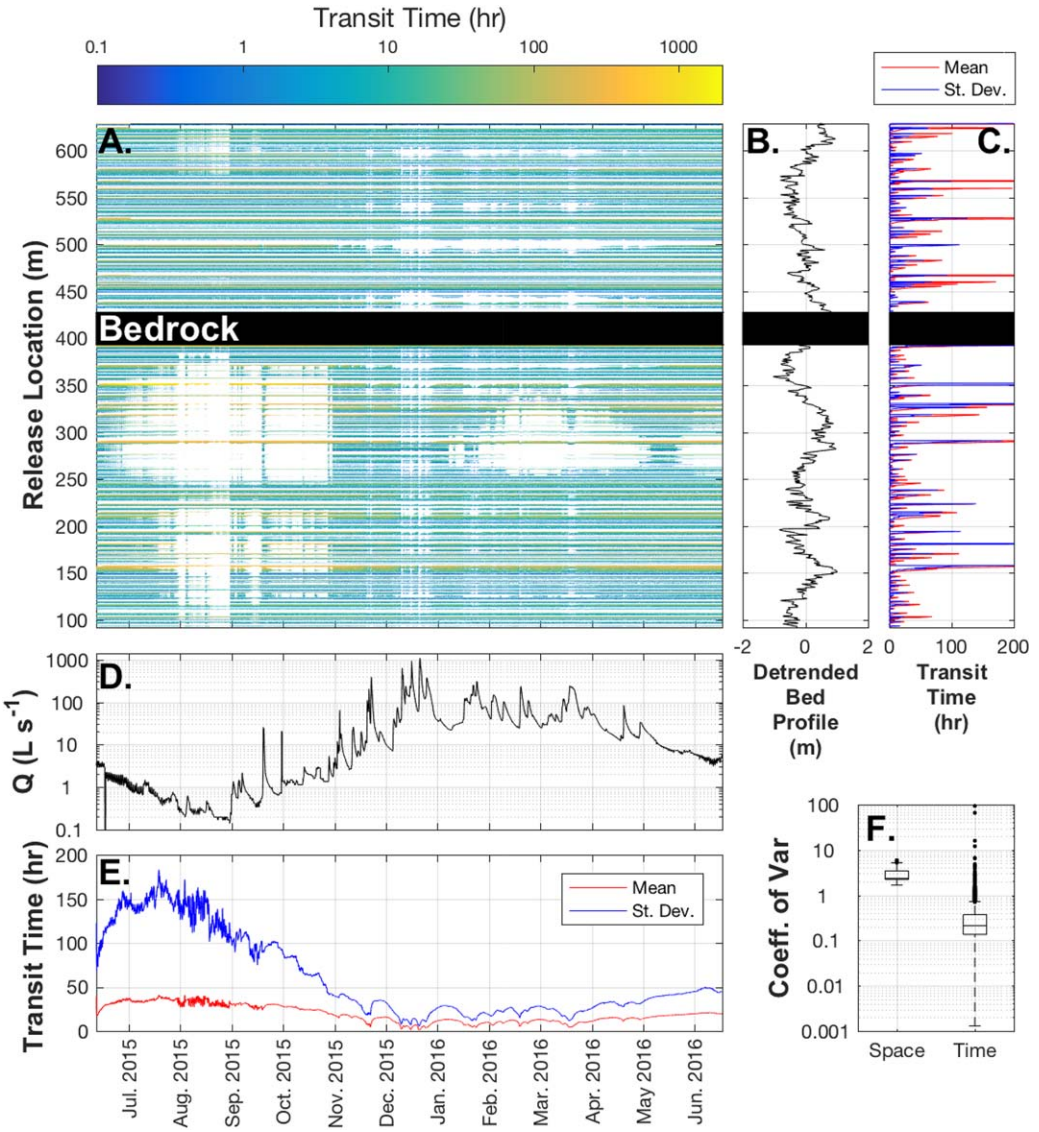

Figure 2. (a) Transit times for each of the >44 million particles tracked. Color denotes transit time; white pixels represent places and times where the streambed was upwelling or unsaturated. The black bar represents an observed bedrock outcrop where no hyporheic flow is simulated. (b) Detrended streambed topography along the study reach. (c) Mean and standard deviation for TTDs calculated every 10 cm release location along the study reach, integrating all time steps (i.e., along a row in plot a). (d) Hydrograph at the WS01 stream gauge. (e) Mean and standard deviation for TTDs calculated every hour through the 1-year study period, integrated along the entire study reach (i.e., down a column in plot a). (f) Boxplot summarizing distributions of the coefficient of variation for the data presented when aggregated through (plot e) space and (plot c) time.

Instantaneous transit time distributions are generally transferable across a broad range of base flow discharges. For all possible pairs of instantaneous TTDs, we find an average RMSE of 0.0091 (median 0.0067; maximum 0.071; minimum 3.2E-4; Supplemental Figure S1). We found that the time elapsed between two instantaneous TTDs is unrelated to the transferability of the TTD in time (supporting information Figure S1A). However, we did find that transferability of instantaneous TTDs was generally more prone to error as differences in discharge increase (supporting information Figure S1B). Finally, we found that transferability of instantaneous TTDs was also prone to large errors with differences in dQ/dt (supporting information Figure S1C). For example, an instantaneous TTD from steady discharge conditions ($dQ/dt = 0$) yielded the highest RMSE when compared to steeply rising or falling discharge conditions.

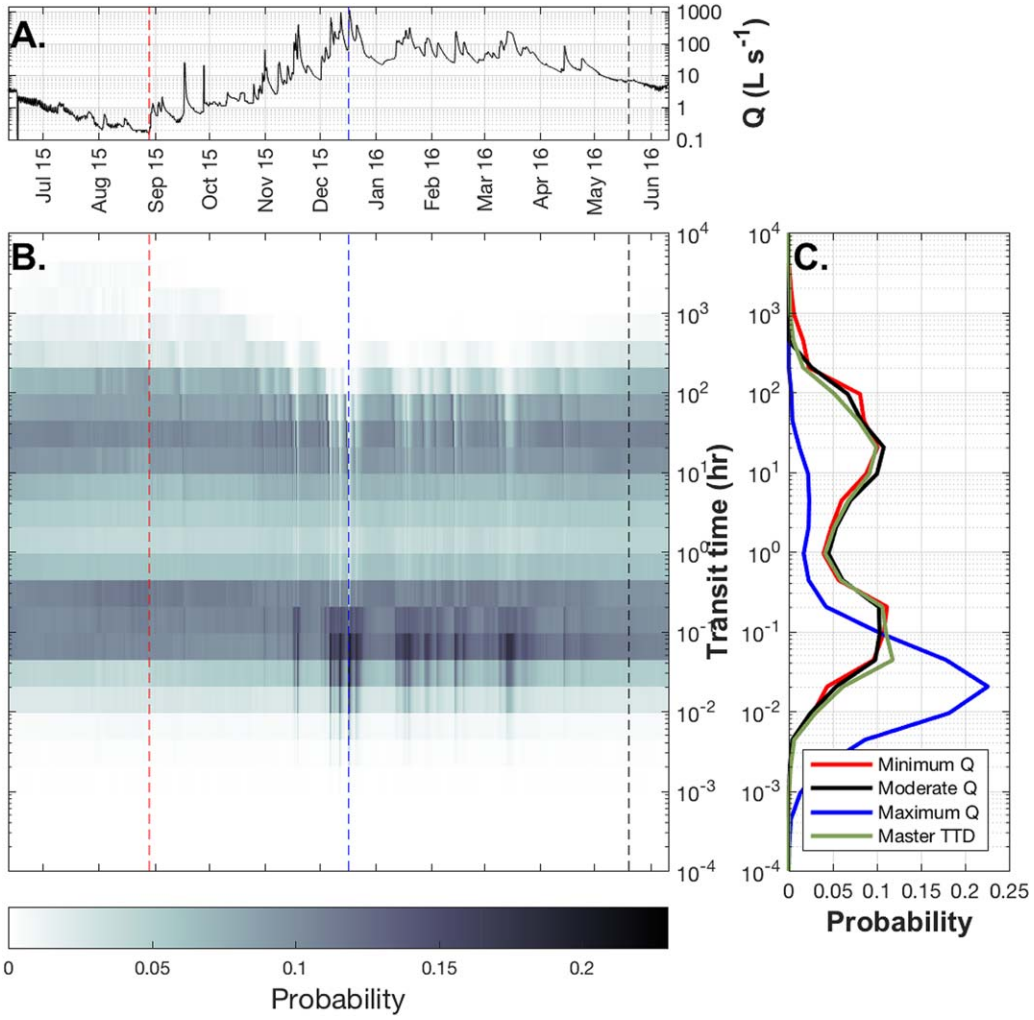

Figure 3. (a) Hydrograph at the Watershed 1 (WS01) stream gauge, with vertical dashed lines denoting the maximum (blue), minimum (red), and an intermediate (black) discharge condition. (b) Instantaneous TTDs constructed from all particles released each hour along the study reach. The pattern of shading moving down a column represents the probability distribution, with darker colors indicating higher probability. (c) Probability distributions associated with the three dashed lines in plots a and b, plus a master TTD constructed from all transit times in the study.

3.2. Spatial Variability in Transit Times

Hyporheic transit times vary with location along the study reach, but are relatively constant through time at any individual location (horizontal bands in Figure 2a). The heterogeneity in transit times among locations along the study reach, averaged over time, ranges from $<$0.01 to 874.6 h (Figure 2c). This heterogeneity arises because the TTDs at a single point reflect the morphology and upwelling conditions at the local particle release location as well as the hydraulics of the broader system through which the particle travels. Most spatially discrete TTDs exhibit narrow ranges through the simulation period, as evidenced by the relatively high probability of narrow ranges of time scales. Thus, the coefficient of variation at individual locations is low, averaging 0.35 (range 0.0013–93.6, median 0.21). Variation in TTDs at a point is generally related to streambed morphology.

3.3. Comparison of Variation in Space and Time

Variation in instantaneous TTDs through time is significantly smaller than the variation in spatially discrete TTDs with location along the reach ($p \ll 0.001$ for one-way ANOVA, Kruskal-Wallis, and Mann-Whitney-Wilcoxson tests on coefficient of variation; Figure 2f). This finding agrees with the steady state results that demonstrated little variation in hyporheic transit times across three different discharge conditions

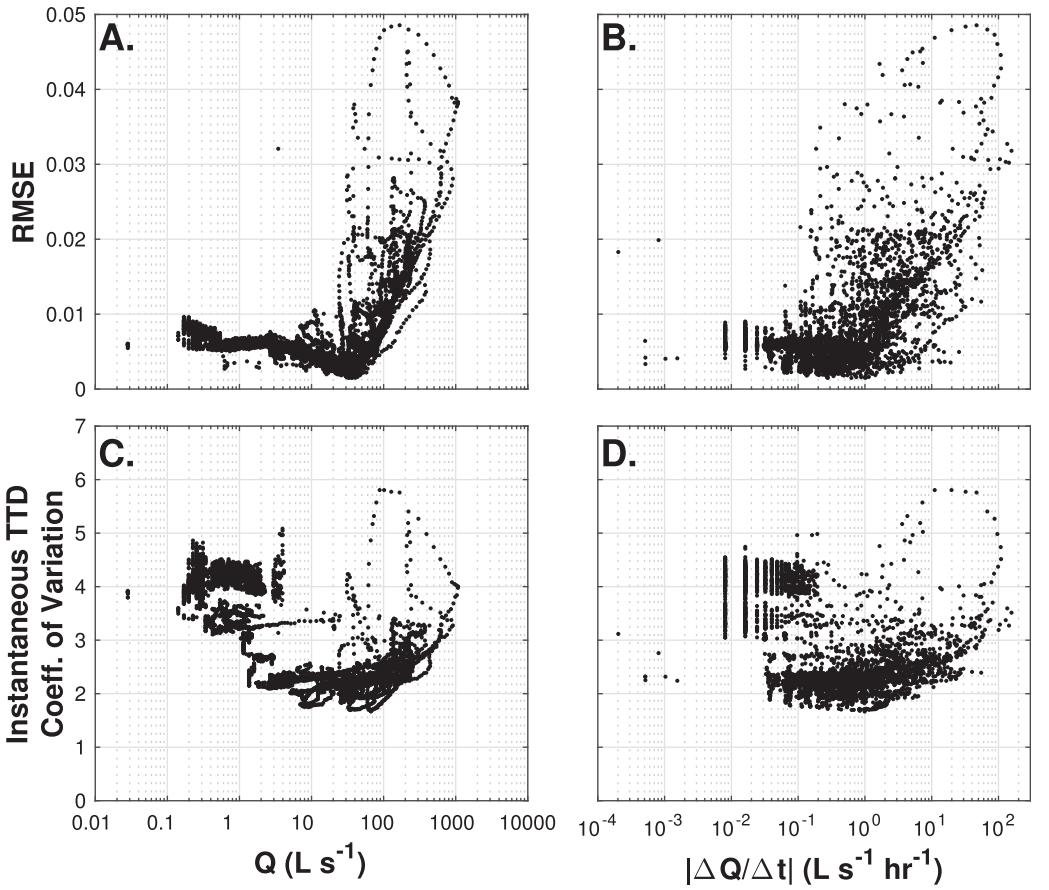

Figure 4. Root mean square error (RMSE; top row) and transit time distribution coefficient of variation (TTD; bottom row) as a function of discharge (left column) and time rate of change of discharge (right column).

(Schmadel et al., 2017). Although we find heterogeneity in spatially discrete TTDs along the study reach, these TTDs are generally consistent through time at individual locations, which Schmadel et al. (2017) attribute to large hydraulic gradients across steep features. The largest changes are associated with the most extreme hydrologic conditions.

3.4. Master Transit Time Distribution Approach

The master TTD reflects all of the particle transit times tabulated from the simulations at all times and at all release locations. The master TTD reflects the bimodal shape of the distribution observed in the instantaneous TTDs (Figure 3c). The master TTD effectively represents the instantaneous TTDs for the most frequent discharge conditions, with overall mean RMSE of 0.0067 (median 0.0058; maximum 0.049, minimum 0.0015; Figures 5a and 5b). The largest errors occurred during the highest stream discharge periods when the instantaneous TTDs became unimodal (Figures 3c and 5c). The maximum deviation between the master TTD and any of the instantaneous TTDs is a deviation in probability of about 20%, reflecting cases where the longest transit times diverge from the master TTD. Overall, error using the master TTD was largest for discharges above about 20 L s^{-1}, and increased as discharge increased (Figure 5c). The master TTD was also most error-prone (i.e., least representative of instantaneous TTDs) during more rapid changes in discharge (Figures 5a and 5b).

3.5. Spatial Averaging of TTDs

Overall, longer study reaches better integrate spatial variation and capture a representative suite of flow paths (Figure 6). Across all discharges, median RMSE decreases from about 0.09 (i.e., an average of 9% error in the TTD across all time scales) for study reaches of 1 m to less than 0.01 for reaches longer than 100 m. The longer reaches are more representative of the complete TTD for the reach because they capture more

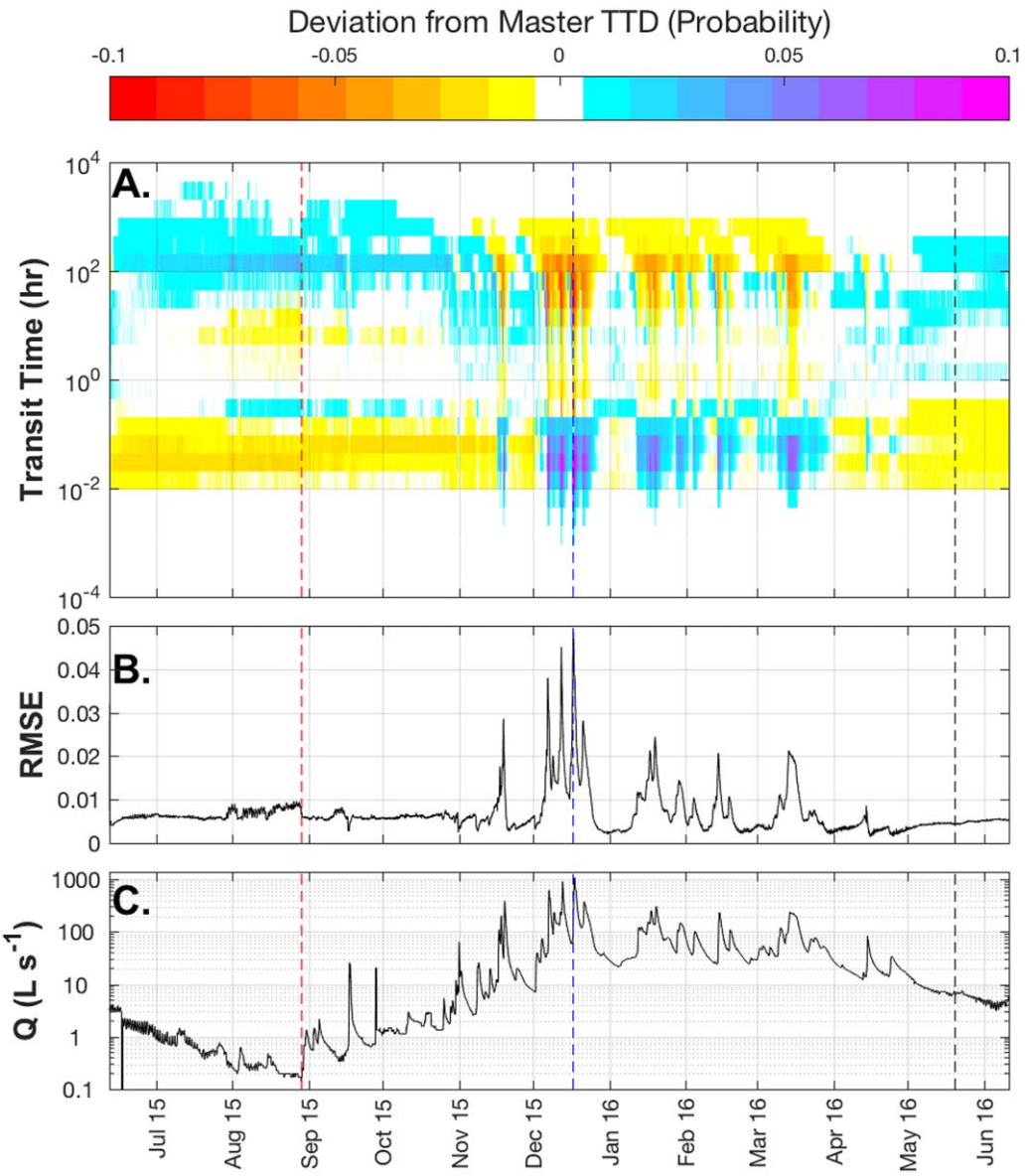

Figure 5. (a) Deviation between the master TTD and instantaneous TTDs for all time steps. (b) RMSE between the master TTD and individual instantaneous TTDs. (c) Hydrograph at the WS01 stream gauge through the 1-year simulation period. Vertical dashed lines in all plots correspond to those in Figure 3. Deviations from the master TTD of less 0.005 are not shown in panel A.

heterogeneity in morphologic features and nested flow paths (i.e., integrating several pool-step features rather than isolating one feature). Shorter reaches are biased toward shorter and faster flow paths. Additionally, longer reaches allow the flow paths that span multiple features to return within the study reach, extending the longer time scales included in the distribution (Figures 6a, 6c, and 6e) and improving the overall representation (decreasing RMSE with increasing length; Figures 6b, 6d, and 6f).

4. Discussion

4.1. How Representative is a Measured TTD of System Behavior at Other Times or Locations?

Many solute tracer studies and modeling efforts have attempted to measure TTDs to describe exchanges between streams and their catchments. These TTDs are most commonly akin to our instantaneous TTDs, where field experiments are integrated in space at a given time of experimentation. An implicit assumption

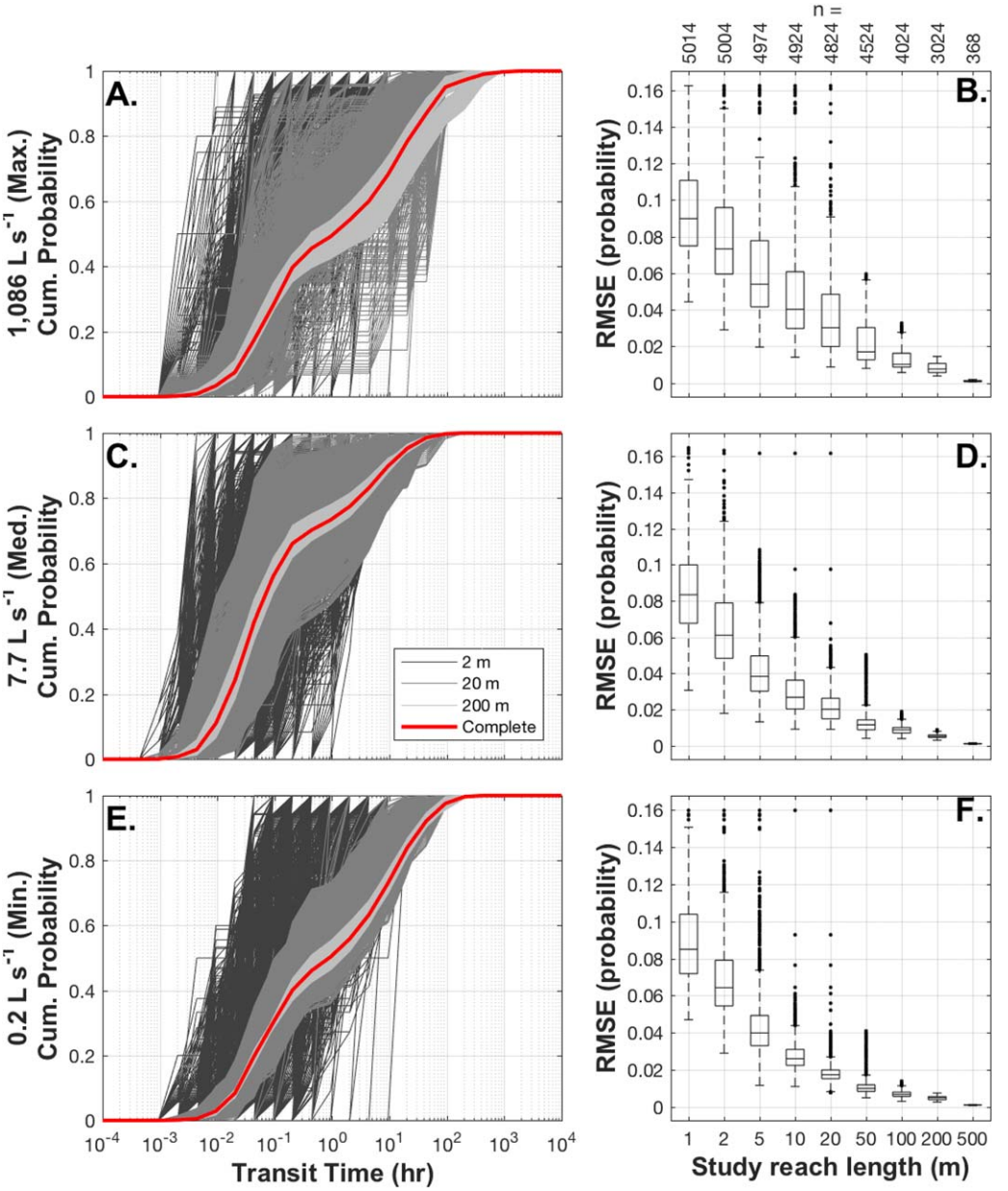

Figure 6. Error between spatial subsets of flow paths and the complete TTD as a function of study reach length (1–500 m) for maximum (plots a and b), median (plots c and d), and minimum (plots e and f) discharge conditions. The left column shows cumulative distributions for all 2, 20, and 200 m distributions along with the complete, entire reach TTD for the time step. The right column shows boxplots of RMSE as a function of spatial window size.

of such field-based efforts, which are time and effort intensive and necessarily limited in scope, is that a measured reach-scale TTD is representative of the system being studied. Indeed, these measured transit times are commonly used as the basis for describing physical transport processes and for subsequent interpretation of additional reactive processes, such as biogeochemical transformations of solutes (e.g., Triska et al., 1989), thermal energy regulation (e.g., Arrigoni et al., 2008), or any other reactive processes occurring along subsurface flow paths (e.g., Gandy et al., 2007; Larson et al., 2013). The results presented here demonstrate that—for our study system—a TTD estimated during steady discharge conditions is likely to be representative of system behavior under a wide range (from low to intermediate discharge) of base flow conditions. This finding is encouraging as significant effort has been focused on reach-scale studies, which integrate spatial heterogeneity at a given time similarly to our instantaneous TTDs.

TTDs at individual locations (spatially discrete and lumped in time) tend to have a low coefficient of variation because transit times do not vary substantially despite the orders-of-magnitude change in discharge. The largest changes are generally associated with a streambed location becoming dry and the flow path "turning off" for a period of time. Spatial heterogeneity in these TTDs is much greater than temporal variability. Consequently, measurement of temporal variability of an individual flow path—for example, by repeated down-well tracer injections (Menichino et al., 2014)—is unlikely to generate a TTD that is representative of the larger reach-scale TTD. Clearly, measuring TTDs at a single well, or from a network of wells, primarily yields flow path-specific information. This is likely the reason that studies seeking to generalize flow path-scale information to reach-scale models struggle to represent the observed, spatially integrated transit times (e.g., Zarnetske et al., 2015).

Instantaneous TTDs are relatively consistent over a wide range of base flow discharges and exhibit a consistent bimodal distribution for all but the most extreme discharge conditions (Figure 3b). Under the most strongly gaining conditions (i.e., fastest time rate of change in discharge at the gauge), the large inflows to the valley bottom are sufficient to force longer time scale down-valley flow paths to upwell, shifting the instantaneous TTD toward the shorter modes. Strongly upwelling conditions are generally associated with the least variable instantaneous TTDs (lowest coefficient of variation), where the longer down-valley mode is truncated. This is consistent with published conceptual and mathematical models (Baxter & Hauer, 2000; Dent et al., 2001; Stonedahl et al., 2010, 2013; Tonina & Buffington, 2009; Winter et al., 1998). In contrast, the lowest discharge conditions are associated with the most variable (i.e., highest coefficient of variation) instantaneous transit time distributions. During the lowest discharge conditions, spatially intermittent surface flow corresponds with more flow paths that travel down-valley below the dry streambed, increasing the representation of the longest flow paths in the probability distribution (Figures 3b and 3c).

The master TTD approach is not a good strategy for flow path-scale interests, such as detailed geochemical processes occurring along a flow path (e.g., Zarnetske et al., 2011). In this application, the integration of space and time to form the master TTD is a hindrance, capturing reach-scale representation at the expense of the granular detail required for interpreting process dynamics. However, the master TTD approach is a reasonable representation of instantaneous TTDs for the reach under most discharge conditions. With exceptions of the highest and lowest discharge conditions, the master TTD exhibits low error. Inversely, most instantaneous TTDs—particularly those collected under steady discharge conditions during intermediate or low base flow—are good approximations of the master TTD. Given this finding, it is reasonable to consider an instantaneous TTD as a feasible first approximation of reach-scale dynamics for most of the year (RMSE less than 1% probability for about 88% of time steps). An additional application of a master TTD would be with respect to the role of subsurface processes through an annual cycle along a study reach. If a process rate remained constant through the year and homogeneous in space, the master TTD could be used to infer the aggregated impact of subsurface flow paths on reach-scale processes. Such an application would also require construction of a TTD using flux-weighting of each particle, which is readily possible using the model results.

Finally, study reaches of 100 m and longer are representative of the distributions of time scales within the study reach, which is in good agreement with typical spatial scales of solute tracer studies in headwater streams (Runkel, 2002; Ward, 2015). This assessment assumes that a solute tracer study can be designed to minimize artificial truncation due to detection limits (i.e., the window of detection problem; Harvey et al., 1996). Furthermore, we note that this finding is unique to our modeled system. Scaling to other systems based on transit times (e.g., standardizing for a uniform travel time as suggested by Schmadel et al., 2016b) or morphology (e.g., standardizing to a fixed number of channel widths; Anderson et al., 2005) could be used to guide the design of comparable tracer studies. Still, our study confirms that typical reaches of 50–200 m that are common in headwater mountain streams are likely reasonable to capture TTDs if the window of detection problem can be overcome with either improved sensitivity to tracers (e.g., using tracers that are detectible at lower concentrations, such as DNA, e.g., Foppen et al., 2011 or fluorescent tracers, e.g., Aubeneau et al., 2015) or by extending the recovered data to complete the TTD (e.g., Drummond et al., 2012).

4.2. Matching Transit Time Distributions to Conditions and Processes of Interest

Key to collecting a meaningful and representative TTD is to match those characterizations to the processes of interest (Hester & Gooseff, 2010, 2011; Ward et al., 2011). Our argument above suggests that a base flow

TTD is reasonably representative of other base flow TTDs and will be useful as a basis to enable estimates of other reactive processes. For example, an instantaneous TTD collected under base flow conditions will likely provide a representative basis for the physical processes associated with estimates of biochemical transformations under similar discharge conditions. However, not all processes of interest are associated with base flow conditions.

One possible application of time-variable TTDs in the river corridor is the mobilization of contaminants from the subsurface to the stream channel in response to storm-melt or snowmelt-generated peak flow events. Consider the role of TTDs in two high-profile cases of pollution of the river corridor. First, the East Fork Poplar Creek (Oak Ridge, TN, USA) drains the US DOE's Oak Ridge Y-12 National Security Complex, the primary site for US manufacture and storage of enriched uranium. Spills, leaks, emissions, and losses of elemental mercury from 1950 to 1963 totaled more than 920 metric tons and resulted in extensive environmental contamination (USDOE, 2013), with the site being placed on the USEPA's Superfund Program's National Priorities List in 1989. At present, the most significant mercury exports from the site are associated with storm events, where Hg stored in the floodplains is mobilized to the stream (Southworth et al., 2010). Second, the remediation plan for the Gold King Mine spill (near Silverton, CO, USA) relies upon a "wait and see" monitoring approach, wherein the responses to snowmelt and storms are key monitoring periods to assess contaminant storage and the system wet-weather loading (USEPA, 2016). This approach is reactionary, requiring monitoring and subsequent action because tools to forecast water quality responses to dynamic hydrological forcing are lacking. In both cases, responses during peak flow periods are critical for predicting system behavior. Unfortunately, these are the conditions where our study demonstrates the least ability to transfer either an instantaneous TTD or master TTD and make accurate predictions.

Observed, instantaneous TTDs are similarly limited in their potential usefulness under the lowest discharge conditions if the stream becomes spatially intermittent. These low-flow conditions represent the times and places where down-valley subsurface flow and/or hyporheic exchange are highest relative to surface flow (Wondzell, 2011). Under these low-discharge conditions, the use of a TTD from higher discharge conditions would underestimate the longest time scale flow paths.

4.3. Hyporheic TTDs Reflect Nested Scales of Exchange Flow Paths Described in Conceptual, Numerical, and Field-Based Studies

Hyporheic exchange flow paths have commonly been conceptualized as occurring at nested scales (Wondzell & Gooseff, 2014), directly paralleling the framework of nested flow paths at local, intermediate, and regional scales by Tóth (1962, 1963). In our simulations, the bimodal, spatially integrated TTDs directly reflect this conceptual model. The faster mode typically occurs at time scales of less than 1 h, reflecting relatively short-distance exchanges driven by steep hydraulic gradients along the longitudinal profile of the stream. The slower mode is typically 10–100 h, reflecting flow paths that span multiple features. These longer flow paths are the characteristic down-valley flow that has been described at the study site (Voltz et al., 2013; Ward et al., 2016, 2017) and other mountain streams (Castro & Hornberger, 1991; Kennedy et al., 1984). Although these nested flow paths are commonly conceptualized and simulated, their documentation in field studies is typically limited to being lumped into "long-term storage" with no defined distribution of time scales.

Based on field studies in this system, Ward et al. (2013a) have described these two modes as short-term storage (those flow paths detectable by solute tracer studies) and long-term storage (those flow paths accounting for mass losses of stream solute tracers). Instantaneous tracer releases (commonly "pulse," "slug," or "gulp" injections) can be interpreted as TTDs. The bias of these methods toward the shortest and fastest flow paths (commonly the "window of detection" problem) is well recognized (Harvey et al., 1996; Wagner & Harvey, 1997). Still, researchers use these studies as the basis for scaling from short study reaches to networks despite a clear recognition that these TTDs are incomplete (Covino et al., 2011; Mallard et al., 2014). As a result, these upscaling strategies fail to account for the longer mode of down-valley transport in the subsurface, which may be important in some systems or for certain applications. For processes whose characteristic time scales are longer (e.g., denitirifcation or respiration along flow paths), these upscaling strategies will bias potential interpretations of ecosystem processes. Possible strategies to more completely describe both fast and slow modes of down-valley transport include the application of models that account for longer-than-observable flow paths through the subsurface (e.g., Ward et al., 2017) or extension of

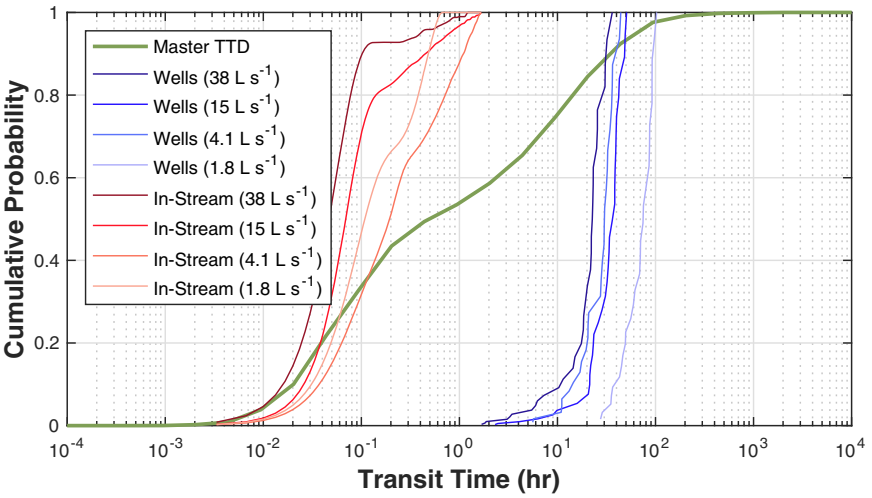

Figure 7. Cumulative distribution of the master TTD (green) in comparison to empirical TTDs derived from solute tracer studies monitoring in-stream (red lines) and in a network of monitoring wells (blue lines) at the field site.

observational data including TTDs (Drummond et al., 2012) or Ranked StoraAge Selection functions (Harman, 2015; Harman et al., 2016). Finally, we note here that the bimodal distribution observed may be unique to this site, where bedrock constraint interacts with stream morphology to set the TTD. Future study in systems with larger alluvial deposits or different morphology will be important to inform TTD dynamics and heterogeneity in other systems.

4.4. Limitations in Model and Field Approaches to Measure TTDs

As simulated, the short time scale TTDs arise due to feature-scale variation in streambed topography and pressure head at the streambed. We acknowledge here there is a nested, smaller-scale of exchange driven by turbulence at the streambed and interactions between in-stream flow fields with cobbles and large woody debris. While these are likely not the dominant drivers of exchange in our study reach (Wondzell & Gooseff, 2014), it is important to note that these finer-scale TTDs were beyond the scope of this study but could be evaluated using hydrostatic and hydrodynamic model comparisons (after Endreny et al., 2011a, 2011b). Intermediate scale TTDs were generally lacking because this high-gradient mountain stream has a relatively linear planform, generally lacking secondary channels, meander bends, and other morphologic features that would generate intermediate scale TTDs. The longest TTDs would be generated by the largest steps in the channel's longitudinal gradient, which are common in this step-pool channel. The largest steps generate the largest hydrostatic gradients, driving at least some hyporheic exchange deep into colluvium and this water must flow along relatively long flow paths to generate the longest proportion of the TTD. In addition to simplifying the processes represented, the model is also limited by the assumptions related to physical setting and structure. For example, the assumption of homogeneous and isotropic porous media simplified flow path geometries that are known to be more complex in heterogeneous sediment (Salehin et al., 2004; Sawyer & Cardenas, 2009). Additionally, the nature of the 2-D profile along the stream centerline omits down-valley flow paths in the valley margins which are known to exist at the site (e.g., Ward et al., 2017).

Very likely, the single most limiting factor in applying the TTD approach will be the ability to simulate or measure an unbiased estimate of the actual TTD. Simulations of TTDs are likely to have substantial limitations due to the inability to accurately characterize heterogeneity in geomorphic setting at fine scales (e.g., subsurface heterogeneity, cobbles on the streambed). Furthermore, models are limited in the processes which can be represented—even advanced feature-scale simulations lack a full two-way coupling of stream turbulence in open channels with hyporheic domains (Cardenas & Wilson, 2007b; Malzone et al., 2016).

The values in the stream and wells span distinctly different time periods because they are sensitive to different suites of flow paths. In field studies, stream solute tracers are perhaps the most common technique to assess exchange between streams and their hyporheic zones (Stream Solute Workshop, 1990), despite their demonstrated bias toward the shortest and fastest flow paths (e.g., Harvey et al., 1996; Harvey & Wagner,

2000; Wagner & Harvey, 1997). The 2012 TTDs derived from stream solute tracer studies clearly demonstrate this bias, with their overall time scales most closely aligned with the shorter mode of transport times in the simulation (Figure 7). However, we note that our model does not simulate in-channel flows so the abundance of short transit times are due to an abundance of short transit time hyporheic flow paths and not in-channel transient storage. In-stream tracer studies reflect the reactively short flow paths that may span just a few features in space, resulting from exchanges due to hydrostatic gradients across steep streambed locations (Wondzell & Gooseff, 2014). In contrast, the monitoring well observations are best aligned with the longer down-valley mode of transport (Figure 7). These findings are consistent with reports by Ward et al. (2012, 2014) who found time scales of down-valley transport in the subsurface were substantially longer than would be expected from in-stream signals alone. These flow paths span many features and are more sensitive to changes in valley width and gradient, governed by Darcy's law applied in the down-valley direction (Ward et al., 2017). Perhaps most promising finding from the comparison of model and field data is the potential to employ multiple methods to collect complimentary data about a system of interest, each of which will have its own strengths and limitations (González-Pinzón et al., 2015).

The monitoring wells with the fastest transit times are those nearest the stream channel, sampling the shorter flow paths that are associated with the feature-scale exchanges (Ward et al., 2017). The master TTD generally represents the scales of exchange measured in the field. The shorter mode that we attribute to feature-scale exchange (10^{-2} to 10^{0} h transit times; Figure 7) are well-aligned with the time scales measured by the stream solute tracers. Thus, our study provides one of the first clear visualizations of which flow paths are measured by stream solute tracers.

5. Conclusions

The overarching goal of this study was to characterize time-variable TTDs at the spatial scale of our study segment, incorporating the hydrological variation occurring over a 1-year period. We expected TTDs to be highly variable in time given the orders-of-magnitude variation in hydrologic forcing (e.g., stream discharge). Instead, we found that segment-scale instantaneous TTDs were nearly constant through the period simulated. The limited variation in time was significantly less than spatial variability along the study segment ($p \ll 0.001$ for one-way ANOVA, Kruskal-Wallis, and Mann-Whitney-Wilcoxson rank sum tests). Furthermore, the near-constant instantaneous TTDs suggest that—contrary to our expectations—the master TTD approach is representative of all but the most extreme low-discharge conditions (e.g., when surface flow becomes spatially intermittent) and high discharge conditions (e.g., when groundwater inflows are strong enough to effectively eliminate down-valley underflow). Understanding the conditions for which a steady state TTD is and is not representative is an important contribution of this study. Finally, we found that an instantaneous TTD collected under one discharge condition is highly transferable in time. However, reaches of 100 m or longer in our system appear to capture reach-representative variation in the TTD. Taken together, results of this study demonstrate that vertical exchange processes in steep, confined headwater mountain streams are generally constant in time and highly heterogeneous in space. Ultimately, we call for improved understanding of how features aggregate and interact at the reach-scale, particularly during periods of dynamic hydrologic forcing, as a requisite step to improved forecasting of ecological functions associated with hyporheic exchange.

Acknowledgments
Tools for spatial data processing and time series analysis were developed by Ward and Schmadel with support provided in part by NSF EAR 1505309 and NSF EAR 1331906. Ward was also supported by NSF EAR 1652293, the Indiana University Office of the Vice Provost for Research, and the Indiana Water Resources Research Center. Field campaigns were funded in part by the Leverhulme International Network's "Where rivers, groundwater and disciplines meet: a hyporheic research network." The authors thank Jase Hixson, Kerry Neil, Stephen Plont, and Brynn O'Donnell for help with data collection. Facilities and additional data were provided by the H.J. Andrews Experimental Forest research program, funded by the NSF's Long-Term Ecological Research Program (NSF DEB 1440409), U.S. Forest Service Pacific Northwest Research Station, and Oregon State University. Any opinions, findings, and conclusions or recommendations expressed in this material are those of the authors and do not necessarily reflect the views of the National Science Foundation, U.S. Forest Service, U.S. Geological Survey, H.J. Andrews Experimental Forest, Oregon State University, or Indiana University. Precipitation, discharge, and spatial data are available from H.J. Andrews Experimental Forest Data Catalog (http://andrewsforest.oregonstate.edu/). The research was conceptualized and written by ASW, NMS, and SMW. NMS led the numerical model development and ASW led the data analysis and writing. Topographic survey data, water level data, and simulation results are available upon request to the corresponding author. The authors report no conflicts of interest.

References

Anderson, J. K., Wondzell, S. M., Gooseff, M. N., & Haggerty, R. (2005). Patterns in stream longitudinal profiles and implications for hyporheic exchange flow at the H. J. Andrews Experimental Forest, Oregon, USA. *Hydrological Processes*, *19*(15), 2931–2949.

Arrigoni, A. S., Poole, G. C., Mertes, L. A. K., O'daniel, S. J., Woessner, W. W., & Thomas, S. A. (2008). Buffered, lagged, or cooled? Disentangling hyporheic influences on temperature cycles in stream channels. *Water Resources Research*, *44*, W09418. https://doi.org/10.1029/2007WR006480

Aubeneau, A. F., Hanrahan, B., Bolster, D., & Tank, J. L. (2015). Substrate size and heterogeneity control anomalous transport in small streams. *Geophysical Research Letters*, *41*, 8335–8341. https://doi.org/10.1002/2014GL061838

Baxter, C. V., & Hauer, F. R. (2000). Geomorphology, hyporheic exchange, and selection of spawning habitat by bull trout (*Salvelinus confluentus*). *Canadian Journal of Fisheries and Aquatic Sciences*, *57*(7), 1470–1481.

Bencala, K. E., Kennedy, V. C., Zellweger, G. W., & Jackman, A. P. (1984). Interactions of solutes and streambed sediment: 1. An experimental analysis of cation and anion transport, *Water Resources Research*, *20*(12), 1797–1803.

Boano, F., Harvey, J. W., Marion, A., Packman, A. I., Revelli, R., Ridolfi, L., & Worman, A. (2014). Hyporheic flow and transport processes: Mechanisms, models, and biogeochemical implications. *Reviews of Geophysics*, *52*, 603–679. https://doi.org/10.1002/2012RG000417

Botter, G., Bertuzzo, E., & Rinaldo, A. (2011). Catchment residence and travel time distributions: The master equation. *Geophysical Research Letters*, *38*, L11403. https://doi.org/10.1029/2011GL047666

Boulton, A. J., Findlay, S., Marmonier, P., Stanley, E. H., & Valett, H. M. (1998). The functional significance of the hyporheic zone in streams and rivers. *Annual Review of Ecology, Evolution, and Systematics*, *29*(1), 59–81.

Brunke, M., Brunke, M., Gonser, T., & Gonser, T. (1997). The ecological significance of exchange processes between rivers and groundwater. *Freshwater Biology*, *37*, 1–33. https://doi.org/10.1046/j.1365-2427.1997.00143.x

Cardenas, M. B., & Wilson, J. L. (2007a). Exchange across a sediment-water interface with ambient groundwater discharge. *Journal of Hydrology*, *346*(3–4), 69–80.

Cardenas, M. B., & Wilson, J. L. (2007b). Hydrodynamics of coupled flow above and below a sediment-water interface with triangular bedforms. *Advances in Water Resources*, *30*(3), 301–313. https://doi.org/10.1016/j.advwatres.2006.06.009

Castro, N. M., & Hornberger, G. M. (1991). Surface-subsurface water interactions in an alluviated mountain stream channel. *Water Resources Research*, *27*(7), 1613–1621.

Cirpka, O. A., Fienen, M. N., Hofer, M., Hoehn, E., Tessarini, A., Kipfer, R., et al. (2007). Analyzing bank filtration by deconvoluting time series of electric conductivity. *Ground Water*, *45*(3), 318–328.

Connor, B. L. O., Hondzo, M., Harvey, J. W., & O'connor, B. L. (2010). Predictive modeling of transient storage and nutrient uptake: Implications for stream restoration. *Journal of Hydraulic Engineering*, *136*, 1018–1032.

Covino, T. P., McGlynn, B. L., & Mallard, J. (2011). Stream-groundwater exchange and hydrologic turnover at the network scale. *Water Resources Research*, *47*, W12521. https://doi.org/10.1029/2011WR010942

D'Angelo, D. J., Webster, J. R., Gregory, S. V., Meyer, J. L., Angelo, A. D. J. D., Webster, J. R., et al. (1993). Transient storage in Appalachian and Cascade Mountain streams as related to hydraulic characteristics. *Journal of the North American Benthological Society*, *12*(3), 223–235. https://doi.org/10.2307/1467457

Dent, C. L., Grimm, N. B., & Fisher, S. G. (2001). Multiscale effects of surface-subsurface exchange on stream water nutrient concentrations. *Journal of the North American Benthological Society*, *20*(2), 162–181.

Drummond, J. D., Covino, T. P., Aubeneau, A. F., Leong, D., Patil, S., Schumer, R., et al. (2012). Effects of solute breakthrough curve tail truncation on residence time estimates: A synthesis of solute tracer injection studies. *Journal of Geophysical Research: Biogeosciences*, *117*, G00N08. https://doi.org/10.1029/2012JG002019

Dudley-Southern, M., & Binley, A. (2015). Temporal responses of groundwater-surface water exchange to successive storm events. *Water Resources Research*, *51*, 1112–1126. https://doi.org/10.1002/2014WR016623

Dyrness, C. T. (1969). *Hydrologic properties of soils on three small watersheds in the western Cascades of Oregon* (USDA For. SERV RES NOTE PNW-111, 17 p.). Portland, OR: Pacific Northwest Forest and Range Experiment Station, U.S. Forest Service.

Elliott, A. H., & Brooks, N. H. (1997a). Transfer of nonsorbing solutes to a streambed with bed forms: Theory. *Water Resources Research*, *33*(1), 123–136.

Elliott, A. H., & Brooks, N. H. (1997b). Transfer of nonsorbing solutes to a streambed with bed forms: Laboratory experiments. *Water Resources Research*, *33*(1), 137–151.

Endreny, T. A., Lautz, L. K., & Siegel, D. I. (2011a). Hyporheic flow path response to hydraulic jumps at river steps: Flume and hydrodynamic models. *Water Resources Research*, *47*, W02517. https://doi.org/10.1029/2009WR008631

Endreny, T. A., Lautz, L. K., & Siegel, D. (2011b). Hyporheic flow path response to hydraulic jumps at river steps: Hydrostatic model simulations. *Water Resources Research*, *47*, W02518. https://doi.org/10.1029/2010WR010014

Findlay, S. (1995). Importance of surface-subsurface exchange in stream ecosystems: The hyporheic zone. *Limnology and Oceanography*, *40*(1), 159–164.

Foppen, J. W., Orup, C., Adell, R., Poulalion, V., & Uhlenbrook, S. (2011). Using multiple artificial DNA tracers in hydrology. *Hydrological Processes*, *25*, 3101–3106. https://doi.org/10.1002/hyp.8159

Fuller, C. C., & Harvey, J. W. (2000). Reactive uptake of trace metals in the hyporheic zone of a mining-contaminated stream, Pinal Creek, Arizona. *Environmental Science and Technology*, *34*(7), 1150–1155.

Gandy, C. J., Smith, J. W. N., & Jarvis, A. P. (2007). Attenuation of mining-derived pollutants in the hyporheic zone: A review. *Science of the Total Environment*, *373*(2–3), 435–446. https://doi.org/10.1016/j.scitotenv.2006.11.004

Gerecht, K. E., Cardenas, M. B., Guswa, A. J., Sawyer, A. H., Nowinski, J. D., & Swanson, T. E. (2011). Dynamics of hyporheic flow and heat transport across a bed-to-bank continuum in a large regulated river. *Water Resources Research*, *47*, W03524. https://doi.org/10.1029/2010WR009794

Gomez-Velez, J. D., & Harvey, J. W. (2014). A hydrogeomorphic river network model predicts where and why hyporheic exchange is important in large basins, *Geophysical Research Letters*, *41*, 6403–6412. https://doi.org/10.1002/2014GL061099

Gomez-Velez, J. D., Harvey, J. W., Cardenas, M. B., & Kiel, B. (2015). Denitrification in the Mississippi River network controlled by flow through river bedforms. *Nature Geoscience*, *8*, 1–8. https://doi.org/10.1038/ngeo2567

González-Pinzón, R., Ward, A. S., Hatch, C. E., Wlostowski, A. N., Singha, K., Gooseff, M. N., et al. (2015). A field comparison of multiple techniques to quantify groundwater–surface-water interactions. *Freshwater Science*, *34*(1), 139–160. https://doi.org/10.1086/679738

Gooseff, M. N., Anderson, J. K., Wondzell, S. M., LaNier, J., & Haggerty, R. (2006). A modelling study of hyporheic exchange pattern and the sequence, size, and spacing of stream bedforms in mountain stream networks, Oregon, USA. *Hydrological Processes*, *20*(11), 2443–2457.

Gooseff, M. N., Wondzell, S. M., Haggerty, R., & Anderson, J. K. (2003). Comparing transient storage modeling and residence time distribution (RTD) analysis in geomorphically varied reaches in the Lookout Creek basin, Oregon, USA. *Advances in Water Resources*, *26*(9), 925–937.

Harman, C. J. (2015). Time-variable transit time distributions and transport: Theory and application to storage-dependent transport of chloride in a watershed. *Water Resources Research*, *51*, 1–30. https://doi.org/10.1002/2014WR015707

Harman, C. J., Ward, A. S., & Ball, A. (2016). How does reach-scale stream-hyporheic transport vary with discharge? Insights from rSAS analysis of sequential tracer injections in a headwater mountain stream. *Water Resources Research*, *52*, 7130–7150. https://doi.org/10.1002/2016WR018832

Harvey, J. W., & Wagner, B. J. (2000). Quantifying hydrologic interactions between streams and their subsurface hyporheic zones. In J. B. Jones & P. J. Mulholland (Eds.), *Streams and ground waters* (pp. 3–44). San Diego, CA: Academic.

Harvey, J. W., Wagner, B. J., & Bencala, K. E. (1996). Evaluating the reliability of the stream tracer approach to characterize stream-subsurface water exchange. *Water Resources Research*, *32*(8), 2441–2451.

Heidbüchel, I., Troch, P. A., Lyon, S. W., & Weiler, M. (2012). The master transit time distribution of variable flow systems. *Water Resources Research*, *48*, W06520. https://doi.org/10.1029/2011WR011293

Hester, E. T., & Gooseff, M. N. (2010). Moving beyond the banks: Hyporheic restoration is fundamental to restoring ecological services and functions of streams. *Environmental Science & Technology*, *44*(5), 1521–1525.

Hester, E. T., & Gooseff, M. N. (2011). Hyporheic restoration in streams and rivers. In A. Simon, S. J. Bennett, & J. M. Castro (Eds.), *Stream restoration in dynamic fluvial systems: Scientif approaches, analyses, and tools. Geophysical monograph series* (Vol. 194, pp. 167–187). Washington, DC: American Geophysical Union.

Kasahara, T., & Wondzell, S. M. (2003). Geomorphic controls on hyporheic exchange flow in mountain streams. *Water Resources Research*, *39*(1), 1005. https://doi.org/10.1029/2002WR001386

Kennedy, V. C., Jackman, A. P., Zand, S. M., Zellweger, G. W., Avanzino, R. J., & Walters, R. A. (1984). Transport and concentration controls for chloride, strontium, potassium and lead in Uvas Creek, a small cobble-bed stream in Santa Clara County, California, USA: 2. Mathematical modeling. *Journal of Hydrology*, *75*(1–4), 67–110.

Kiel, B., & Cardenas, M. (2014). Lateral hyporheic exchange throughout the Mississippi River network. *Nature Geoscience*, *7*, 413–417. https://doi.org/10.1038/ngeo2157

Krause, S., Hannah, D. M., Fleckenstein, J. H., Heppell, C. M., Kaeser, D., Pickup, R., et al. (2011). Inter-disciplinary perspectives on processes in the hyporheic zone. *Ecohydrology*, *4*(4), 481–499.

Larson, L. N., Fitzgerald, M., Singha, K., Gooseff, M. N., Macalady, J. L., & Burgos, W. (2013). Hydrogeochemical niches associated with hyporheic exchange beneath an acid mine drainage-contaminated stream. *Journal of Hydrology*, *501*, 163–174. https://doi.org/10.1016/j.jhydrol.2013.08.007

Mallard, J., McGlynn, B., & Covino, T. P. (2014). Lateral inflows, stream-groundwater exchange, and network geometry influence stream-water composition. *Water Resources Research*, *50*, 4603–4623. https://doi.org/10.1002/2013WR014222

Malzone, J. M., Lowry, C. S., & Ward, A. S. (2016). Response of the hyporheic zone to transient groundwater fluctuations on the annual and storm event time scales. *Water Resources Research*, *52*, 5301–5321. https://doi.org/10.1002/2014WR015716

McGuire, K. J., & McDonnell, J. J. (2006). A review and evaluation of catchment transit time modeling. *Journal of Hydrology*, *330*(3–4), 543–563. https://doi.org/10.1016/j.jhydrol.2006.04.020

Menichino, G. T., Ward, A. S., & Hester, E. T. (2014). Macropores as preferential flow paths in meander bends. *Hydrological Processes*, *28*(3), 482–495. https://doi.org/10.1002/hyp.9573

Merill, L., & Tonjes, D. J. (2014). A review of the hyporheic zone, stream restoration, and means to enhance denitrification. *Critical Reviews in Environmental Science and Technology*, *44*(21), 2337–2379. https://doi.org/10.1080/10643389.2013.829769

Mualem, Y. (1976). A new model for predicting the hydraulic conductivity of unsaturated porous media. *Water Resources Research*, *12*(3), 513–522.

Packman, A. I., & Bencala, K. E. (2000). Modeling surface-subsurface hydrological interactions. In J. B. Jones & P. J. Mulholland (Eds.), *Streams and ground waters* (pp. 45–80). San Diego, CA: Academic.

Packman, A. I., & Salehin, M. (2003). Relative roles of stream flow and sedimentary conditions in controlling hyporheic exchange. *Hydrobiologia*, *494*(1), 291–297.

Packman, A. I., Salehin, M., & Zaramella, M. (2004). Hyporheic exchange with gravel beds: Basic hydrodynamic interactions and bedform-induced advective flows. *Journal of Hydraulic Engineering*, *130*, 647–656. https://doi.org/10.1061/(ASCE)0733-9429(2004)130:7(647)

Payn, R. A., Gooseff, M. N., Benson, D. A., Cirpka, O. A., Zarnetske, J. P., Bowden, W. B., et al.(2008). Comparison of instantaneous and constant-rate stream tracer experiments through parametric analysis of residence time distributions. *Water Resources Research*, *44*, W06404. https://doi.org/10.1029/2007WR006274

Payn, R. A., Gooseff, M. N., McGlynn, B. L., Bencala, K. E., & Wondzell, S. M. (2009). Channel water balance and exchange with subsurface flow along a mountain headwater stream in Montana, United States. *Water Resources Research*, *45*, W11427. https://doi.org/10.1029/2008WR007644

Richards, L. A. (1931). Capillary conduction of liquids through porous mediums. *Journal of Applied Physics*, *1*(5), 318–333.

Rinaldo, A., Beven, K. J., Bertuzzo, E., Nicotina, L., Davies, J., Fiori, A., et al. (2011). Catchment travel time distributions and water flow in soils. *Water Resources Research*, *47*, W07537. https://doi.org/10.1029/2011WR010478

Runkel, R. L. (2002). A new metric for determining the importance of transient storage. *Journal of the North American Benthological Society*, *21*(4), 529–543.

Ryan, R. J., Packman, A. I., & Welty, C. (2004). Estimation of solute transport and storage parameters in a stream with anthropogenically produced unsteady flow and industrial bromide input. *Water Resources Research*, *40*, W01602. https://doi.org/10.1029/2003WR002458

Salehin, M., Packman, A. I., & Paradis, M. (2004). Hyporheic exchange with heterogeneous streambeds: Laboratory experiments and modeling. *Water Resources Research*, *40*, W11504. https://doi.org/10.1029/2003WR002567

Sawyer, A. H., & Cardenas, M. B. (2009). Hyporheic flow and residence time distributions in heterogeneous cross-bedded sediment. *Water Resources Research*, *45*, W08406. https://doi.org/10.1029/2008WR007632

Sawyer, A. H., Edmonds, D. A., & Knights, D. (2015). Surface water-groundwater connectivity in deltaic distributary channel networks. *Geophysical Research Letters*, *42*, 10299–10306. https://doi.org/10.1002/2015GL066156

Schmadel, N. M., Ward, A. S., Kurz, M. J., Fleckenstein, J. H., Zarnetske, J. P., Hannah, D. M., et al. (2016b). Stream solute tracer timescales changing with discharge and reach length confound process interpretation. *Water Resources Research*, *52*, 3227–3245. https://doi.org/10.1002/2015WR018062

Schmadel, N. M., Ward, A. S., Lowry, C. S., & Malzone, J. M. (2016a). Hyporheic exchange controlled by dynamic hydrologic boundary conditions. *Geophysical Research Letters*, *43*, 4408–4417. https://doi.org/10.1002/2016GL068286

Schmadel, N. M., Ward, A. S., & Wondzell, S. M. (2017). Hydrologic controls on hyporheic exchange in a headwater mountain stream. *Water Resources Research*, *53*, 6260–6278. https://doi.org/10.1002/2017WR020576

Schwanghart, W., & Kuhn, N. J. (2010). TopoToolbox: A set of Matlab functions for topographic analysis. *Environmental Modelling & Software*, *25*(6), 770–781. https://doi.org/10.1016/j.envsoft.2009.12.002

Schwanghart, W., & Scherler, D. (2014). Short communication: TopoToolbox 2 - MATLAB-based software for topographic analysis and modeling in Earth surface sciences. *Earth Surface Dynamics*, *2*(1), 1–7. https://doi.org/10.5194/esurf-2-1-2014

Seibert, J., & McGlynn, B. L. (2007). A new triangular multiple flow direction algorithm for computing upslope areas from gridded digital elevation models. *Water Resources Research*, *43*, W04501. https://doi.org/10.1029/2006WR005128

Southworth, G., Greeley, M., Peterson, M., Lowe, K., & Ketelle, R. (2010). *Sources of mercury to east fork poplar creek downstream from the Y-12 National Security Complex: Inventories and export rates* (ORNL/TM-2009/231). Oak Ridge, TN: Oak Ridge National Laboratory.

Spies, T. (2016, 18 August). *LiDAR data (August 2008) for the Andrews Experimental Forest and Willamette National Forest study areas*. Corvalliss, OR: Long-term Ecological Research, Forest Science Data Bank [Database]. Retrieved from http://andrewsforest.oregonstate.edu/data/abstract.cfm?dbcode=GI010

Stanford, J. A., & Ward, J. V. (1993). An ecosystem perspective of alluvial rivers: Connectivity and the hyporheic corridor. *Journal of the North American Benthological Society*, *12*(1), 48–60.

Stonedahl, S. H., Harvey, J. W., & Packman, A. I. (2013). Interactions between hyporheic flow produced by stream meanders, bars, and dunes. *Water Resources Research*, *49*, 5450–5461. https://doi.org/10.1002/wrcr.20400

Stonedahl, S. H., Harvey, J. W., Wörman, A., Salehin, M., & Packman, A. I. (2010). A multiscale model for integrating hyporheic exchange from ripples to meanders. *Water Resources Research*, *46*, W12539. https://doi.org/10.1029/2009WR008865

Storey, R. G., Howard, K. W. F., & Williams, D. D. (2003). Factors controlling riffle-scale hyporheic exchange flows and their seasonal changes in a gaining stream: A three-dimensional groundwater flow model. *Water Resources Research*, *39*(2), 1034. https://doi.org/10.1029/2002WR001367

Stream Solute Workshop (1990). Concepts and methods for assessing solute dynamics in stream ecosystems. *Journal of the North American Benthological Society*, *9*(2), 95–119.

Swanson, F. J., & James, M. E. (1975). *Geology and geomorphology of the H.J. Andrews Experimental Forest, western Cascades, Oregon*, Portland, OR: U.S. Department of Agriculture, Forest Service, Pacific Northwest Forest and Range Experiment Station.

Swanson, F. J., & Jones, J. A. (2002). Geomorphology and hydrology of the H.J. Andrews Experimental Forest, Blue River, Oregon. In *Field guide to geologic processes in Cascadia*. Oregon Department of Geology and Mineral Industries, Special Paper 36.

Tonina, D., & Buffington, J. M. (2009). Hyporheic exchange in mountain rivers. I: Mechanics and environmental effects. *Geography Compass*, *3*(3), 1063–1086. https://doi.org/10.1111/j.1749-8198.2009.00226.x

Tóth, J. (1962). A theory of groundwater motion in small drainage basins in central Alberta, Canada. *Journal of Geophysical Research*, *67*(11), 4375–4387.

Tóth, J. (1963). A theoretical analysis of groundwater flow in small drainage basins. *Journal of Geophysical Research*, *68*(16), 4795–4812. https://doi.org/10.1029/JZ068i016p04795

Triska, F. J., Kennedy, V. C., Avanzino, R. J., Zellweger, G. W., & Bencala, K. E. (1989). Retention and transport of nutrients in a third-order stream in Northwestern California: Hyporheic processes. *Ecology*, *70*(6), 1893–1905.

USDOE (2013). *Strategic plan for mercury remediation at the Y-12 National Security Complex* (DOE/OR/01–2605&D). Oak Ridge, TN: Oak Ridge National Laboraotry.

USEPA (2016). *Post-gold king mine release incident conceptual monitoring plan for surface water, sediments and biology*, March 2016. Retrieved from https://www.epa.gov/sites/production/files/2016-03/documents/post-gkm-final-conceptual-monitoring-plan_2016_03_24_16.pdf

Valett, H. M., Dahm, C. N., Campana, M. E., Morrice, J. A., Baker, M. A., & Fellows, C. S. (1997). Hydrologic influences on groundwater-surface water ecotones: Heterogeneity in nutrient composition and retention. *Journal of the North American Benthological Society*, *16*, 239–247.

Van Genuchten, M. (1980). A closed-form equation for predicting the hydraulic conductivity of unsaturated soils. *Soil Science Society of America Journal*, *44*(5), 892–898.

Vaux, W. G. (1968). Intragravel flow and interchange of water in a streambed. *Fishery Bulletin*, *66*(3), 479–489.

Voltz, T. J., Gooseff, M. N., Ward, A. S., Singha, K., Fitzgerald, M., & Wagener, T. (2013). Riparian hydraulic gradient and stream-groundwater exchange dynamics in steep headwater valleys. *Journal of Geophysical Research: Earth Surface*, *118*, 953–969. https://doi.org/10.1002/jgrf.20074

Wagner, B. J., & Harvey, J. W. (1997). Experimental design for estimating parameters of rate-limited mass transfer: Analysis of stream tracer studies. *Water Resources Research*, *33*(7), 1731–1741.

Ward, A. S. (2015). The evolution and state of interdisciplinary hyporheic research. *Wiley Interdisciplinary Reviews: Water*, *3*(1), 83–103. https://doi.org/10.1002/wat2.1120

Ward, A. S., Fitzgerald, M., Gooseff, M. N., Voltz, T. J., Binley, A. M., & Singha, K. (2012). Hydrologic and geomorphic controls on hyporheic exchange during base flow recession in a headwater mountain stream. *Water Resources Research*, *48*, W04513. https://doi.org/10.1029/2011WR011461

Ward, A. S., Gooseff, M. N., Fitzgerald, M., Voltz, T. J., & Singha, K. (2014). Spatially distributed characterization of hyporheic solute transport during baseflow recession in a headwater mountain stream using electrical geophysical imaging. *Journal of Hydrology*, *517*, 362–377. https://doi.org/10.1016/j.jhydrol.2014.05.036

Ward, A. S., Gooseff, M. N., & Johnson, P. A. (2011). How can subsurface modifications to hydraulic conductivity be designed as stream restoration structures? Analysis of Vaux's conceptual models to enhance hyporheic exchange. *Water Resources Research*, *47*, W08512. https://doi.org/10.1029/2010WR010028

Ward, A. S., Gooseff, M. N., & Singha, K. (2013b). How does subsurface characterization affect simulations of hyporheic exchange? *Ground Water*, *51*(1), 14–28. https://doi.org/10.1111/j.1745-6584.2012.00911.x

Ward, A. S., Gooseff, M. N., Voltz, T. J., Fitzgerald, M., Singha, K., & Zarnetske, J. P. (2013a). How does rapidly changing discharge during storm events affect transient storage and channel water balance in a headwater mountain stream? *Water Resources Research*, *49*, 5473–5486. https://doi.org/10.1002/wrcr.20434

Ward, A. S., Payn, R. A., Gooseff, M. N., McGlynn, B. L., Bencala, K. E., Kelleher, C. A., et al. (2013c). Variations in surface water-ground water interactions along a headwater mountain stream: Comparisons between transient storage and water balance analyses. *Water Resources Research*, *49*, 3359–3374. https://doi.org/10.1002/wrcr.20148

Ward, A. S., Schmadel, N. M., Wondzell, S. M., Gooseff, M. N., & Singha, K. (2017). Dynamic hyporheic and riparian flow path geometry through base flow recession in two headwater mountain streamcorridors. *Water Resources Research*, *53*, 3988–4003. https://doi.org/10.1002/2016WR019875

Ward, A. S., Schmadel, N. M., Wondzell, S. M., Harman, C. J., Gooseff, M. N., & Singha, K. (2016). Hydrogeomorphic controls on hyporheic and riparian transport in two headwater mountain streams during base flow recession. *Water Resources Research*, *52*, 1479–1497. https://doi.org/10.1002/2015WR018225

Winter, T. C., Harvey, J. W., Franke, O. L., & Alley, W. M. (1998). *Ground water and surface water: A single resource* (U.S. Geological Survey Circular 1139).

Wondzell, S. M. (2006). Effect of morphology and discharge on hyporheic exchange flows in two small streams in the Cascade Mountains of Oregon, USA. *Hydrological Processes*, *20*(2), 267–287.

Wondzell, S. M. (2011). The role of the hyporheic zone across stream networks. *Hydrological Processes*, *25*(22), 3525–3532. https://doi.org/10.1002/hyp.8119

Wondzell, S. M., & Gooseff, M. N. (2014). Geomorphic controls on hyporheic exchange across scales: Watersheds to particles. In J. Schroder & E. Wohl (Eds.), *Treatise on geomorphology* (Vol. 9, pp. 203–218). San Diego, CA: Academic Press.

Wondzell, S. M., & Gooseff, M. N. (2013). 9.13 Geomorphic controls on hyporheic exchange across scales: Watersheds to particles. In Shroder, J. F. (Ed.), *Treatise on geomorphology* (pp. 203–218). San Diego, CA: Academic Press.

Wondzell, S. M., LaNier, J., & Haggerty, R. (2009). Evaluation of alternative groundwater flow models for simulating hyporheic exchange in a small mountain stream. *Journal of Hydrology*, *364*(1–2), 142–151.

Wright, K. K., Baxter, J. L. & Li, (2005). Restricted hyporheic exchange in an alluvial river system: Implications for theory and management. *Journal of the North American Benthological Society*, *24*(3), 447–460.

Zarnetske, J. P., Haggerty, R., & Wondzell, S. M. (2015). Coupling multiscale observations to evaluate hyporheic nitrate removal at the reach scale. *Freshwater Science*, *34*(1), 172–186. https://doi.org/10.1086/680011

Zarnetske, J. P., Haggerty, R., Wondzell, S. M., & Baker, M. A. (2011). Dynamics of nitrate production and removal as a function of residence time in the hyporheic zone. *Journal of Geophysical Research*, *116*, G01025. https://doi.org/10.1029/2010JG001356

Zhou, D., & Mendoza, C. (1993). Flow through porous bed of turbulent stream. *Journal of Engineering Mechanics*, *119*(2), 365–383.